



## Study of molecular motion by $^1\text{H}$ NMR relaxation in ferroelectric $\text{LiH}_3(\text{SeO}_3)_2$ , $\text{Li}_2\text{SO}_4\cdot\text{H}_2\text{O}$ , and $\text{LiN}_2\text{H}_5\text{SO}_4$ single crystals

Sung Soo Park\*

Samsung Advanced Institute of Technology (SAIT), Samsung Ro 130, Suwon, Kyeonggi-Do, 16678, Korea

Received Jan 15, 2016; Revised Feb 4, 2016; Accepted Feb 19, 2016

**Abstract** The proton NMR line widths and spin-lattice relaxation rates,  $T_1^{-1}$ , of ferroelectric  $\text{LiH}_3(\text{SeO}_3)_2$ ,  $\text{Li}_2\text{SO}_4\cdot\text{H}_2\text{O}$ , and  $\text{LiN}_2\text{H}_5\text{SO}_4$  single crystals were measured as a function of temperature. The line width measurements reveal rigid lattice behavior of all the crystals at low temperatures and line narrowing due to molecular motion at higher temperatures. The temperature dependences of the proton  $T_1^{-1}$  for these crystals exhibit maxima, which are attributed to the effects of molecular motion by the Bloembergen - Purcell - Pound theory. The activation energies for the molecular motions of  $^1\text{H}$  in these crystals were obtained. From these analysis,  $^1\text{H}$  in  $\text{LiH}_3(\text{SeO}_3)_2$  undergoes molecular motion more easily than  $^1\text{H}$  in  $\text{LiN}_2\text{H}_5\text{SO}_4$  and  $\text{Li}_2\text{SO}_4\cdot\text{H}_2\text{O}$  crystals.

**Keywords** Ferroelectrics, Crystal growth, Nuclear magnetic resonance, Ferroelectricity, Crystal growth, Nuclear magnetic resonance and relaxation

### Introduction

Proton conducting solids have been attracting a great deal of attention, because they are considered as promising materials for a wide variety of electrochemical devices such as fuel cells and proton

batteries, solid state dehumidifiers, solar energy storage and electrochromic display devices.<sup>1</sup> Proton conduction occurs in several types of materials, including many hydrogen-bonded systems. In some ferroelectric hydrogen-bonded crystals, superionic conductivity has been discovered. Compounds with the  $\text{LiH}_3(\text{SeO}_3)_2$ ,  $\text{Li}_2\text{SO}_4\cdot\text{H}_2\text{O}$ , and  $\text{LiN}_2\text{H}_5\text{SO}_4$  belongs to a family of hydrogen-bonded crystals.

The effects of nuclear motion on the magnetic resonance line widths and relaxation times of nuclear spin systems have been widely used in studies of various types of atomic motions in crystals. It is commonly held that a good deal of information regarding the structures and internal motions of solids can be obtained by using nuclear magnetic resonance (NMR) techniques.<sup>2-4</sup> A prominent feature of the solids studied in this manner is that the protons act as resonant nuclei and that variations of their relaxation times with temperature can be used to detect ionic motion. From relaxation time measurements, it has been found that at temperatures in the neighborhood of compounds' phase transition temperatures, both the slope and the actual value of the relaxation time plotted as a function of temperature undergo abrupt changes;<sup>5</sup> it was concluded that a change in molecular motion accompanied the phase change in each case. This method is particularly suited to the study of the

\* Address correspondence to: **Sung Soo Park**, SAIT, Samsung Ro 130, Suwon, Kyeonggi-Do, 16678, Korea, Tel: +82-(0)10-7122-6574; E-mail: sspark1006@gmail.com \* Current Address: Baeksan 607-1502, Yaptap-ro 124, Bundanggu, Seongnam, Kyunggi-do, Korea, 13517

rotational and vibrational properties of ionic groups that contain nuclei with spin  $1/2$ .<sup>6</sup> Most of these experiments have been considered in the framework of the Bloembergen-Purcell-Pound (BPP) theory.<sup>7</sup> The mathematical model used in these studies to convert between the relaxation time,  $T_1$ , and the correlation time,  $\tau_c$ , characteristic of the molecular motion was the model introduced by the BPP theory.<sup>7</sup> This study reports the determination of molecular motion from the line widths and spin-lattice relaxation rates,  $T_1^{-1}$ , for  $^1\text{H}$  in  $\text{LiH}_3(\text{SeO}_3)_2$ ,  $\text{Li}_2\text{SO}_4\cdot\text{H}_2\text{O}$ , and  $\text{LiN}_2\text{H}_5\text{SO}_4$  single crystals grown using the slow evaporation method. Our main intentions were to obtain quantitative activation energies and to determine the types of motions that govern the relaxation processes in these crystals. Based on our  $^1\text{H}$  NMR data, we strove in particular to determine the role of the protons in these processes. Although  $^1\text{H}$  NMR results for two of these crystals have been reported previously, in this study we compared the molecular motions of H in the three crystals by using these  $^1\text{H}$  NMR results. The  $^1\text{H}$  NMR data for  $\text{LiH}_3(\text{SeO}_3)_2$  single crystal used here are reported, and a new result.

### Experimental Methods

$\text{LiH}_3(\text{SeO}_3)_2$  single crystals were grown from an aqueous solution of  $\text{Li}_2\text{CO}_3$  and  $\text{H}_2\text{SeO}_3$  in a stoichiometric molar ratio of 1:3. And, crystals of lithium sulfate monohydrate,  $\text{Li}_2\text{SO}_4\cdot\text{H}_2\text{O}$ , were grown at room temperature from an aqueous solution prepared using analytical grade reagents. Crystals of lithium hydrazinium sulfate,  $\text{LiN}_2\text{H}_5\text{SO}_4$ , were grown from an aqueous solution of reagent grade  $\text{Li}_2\text{CO}_3$  and  $\text{N}_2\text{H}_6\text{SO}_4$  by using slow evaporation. The three crystals were colorless and transparent.

The spectra were obtained at the Larmor frequency,  $\omega_0/2\pi=44.55$  MHz ( $B=1.05$  Tesla), of a pulse NMR spectrometer by using a solid echo pulse sequence,  $(\pi/2-t-\pi/2)$  to eliminate artifacts due to probe ringing. The  $\pi/2$  pulse width was 5  $\mu\text{s}$ , and the pulse separation  $\tau$  was 40  $\mu\text{s}$ . The sample temperature was maintained at a constant value by controlling the helium gas flow and the heater current, giving an accuracy of  $\pm 0.1$  K.

### Results

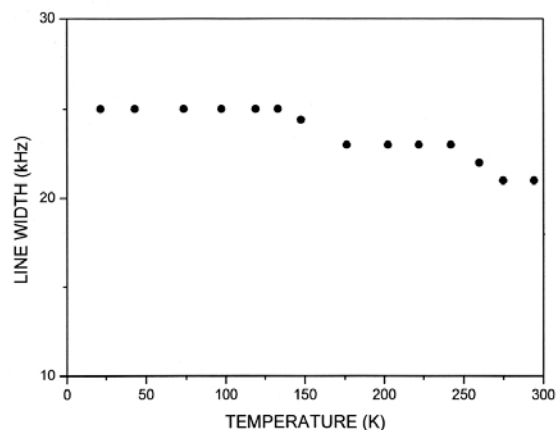


**Figure 1.**  $^1\text{H}$  NMR line-width as a function of temperature for a  $\text{LiH}_3(\text{SeO}_3)_2$  single crystal

*LiH<sub>3</sub>(SeO<sub>3</sub>)<sub>2</sub> single crystals*-The FWHM (full width at half maximum) of the NMR line width for  $^1\text{H}$  in  $\text{LiH}_3(\text{SeO}_3)_2$  as a function of the temperature is measured, and in the experimental temperature range, the line width is nearly constant within the range 21 to 25 kHz as shown in Fig. 1, and has a Lorentzian shape.

The proton spin-lattice relaxation rate was measured in the temperature range 20–300 K. The spin-lattice relaxation time,  $T_1$ , was measured by applying a solid echo pulse sequence, and the nuclear magnetization  $M(t)$  of  $^1\text{H}$  at time  $t$  after the  $\pi/2$  pulse was determined from the saturation recovery pulse, sequence following the pulse. The recovery trace of magnetization of the crystals was measured at several different temperatures. The recovery traces of  $^1\text{H}$  nucleus show a single exponential function. Thus, the spin-lattice relaxation time was determined by fitting it into the recovery pattern given by the following equation<sup>8-10</sup>

$$M(\infty) - M(t) = M(\infty) \exp(-t/T_1) \quad (1)$$

Where  $M(t)$  is the nuclear magnetization at time  $t$ . The relaxation rate,  $1/T_1$ , in eq. (1) was determined directly from the slope of the log  $[M(\infty)-M(t)] / M(\infty)$  versus time  $t$  plot. The proton spin-lattice relaxation rates,  $T_1^{-1}$ , for single crystals of  $\text{LiH}_3(\text{SeO}_3)_2$  are shown in Fig. 2. The relaxation rate

for the  $^1\text{H}$  nucleus undergoes a remarkable change near 242 K. No phase transition exists in this temperature range. In the temperature range 170–300 K, the spin-lattice relaxation rate has a maximum value of  $1.23 \text{ s}^{-1}$  (Fig. 2 inset).

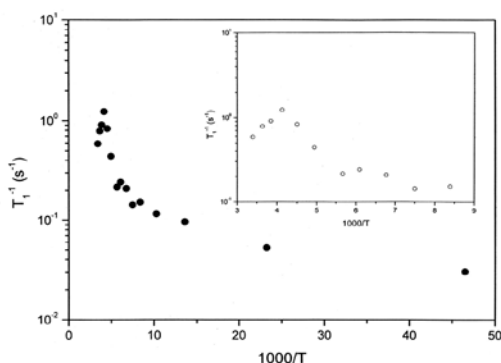


**Figure 2.** Temperature dependence of the spin-lattice relaxation rate,  $T_1^{-1}$ , for  $^1\text{H}$  in a  $\text{LiH}_3(\text{SeO}_3)_2$  single crystal.

There is a well-developed  $T_1^{-1}$  maximum with an exponential on both sides of the maximum, as predicted by the BPP theory of relaxation. Previous studies have reported that the temperature dependence of  $T_1^{-1}$  for  $\text{LiH}_3(\text{SeO}_3)_2$  does not follow a well-defined BPP function.<sup>9</sup> This feature of  $T_1$  indicates that distinct molecular motion is present. The form of the proton  $T_1^{-1}$  vs. inverse temperature curve leads us to believe that the relaxation process is caused by the molecular motion. The  $T_1$  values can be related to corresponding values of the rotational correlation time,  $\tau_c$ , the rotational correlation time being the length of time that a molecule remains in a given state before the molecule reorients. As such,  $\tau_c$  is a direct measure of the rate of motion. The experimental value of  $T_1$  can be expressed in terms of an isotropic correlation time  $\tau_c$  for molecular motions by using the BPP function.<sup>7</sup> According to the BPP theory,  $T_1$  for the spin-lattice interaction in the case of random motion is given by<sup>12,13</sup>

$$T_1^{-1} = 9/10(\gamma^2 \hbar / r^3)^2 [\tau_c / (1 + \omega_0^2 \tau_c^2) + 4\tau_c / (1 + 4\omega_0^2 \tau_c^2)]. \quad (2)$$

Here,  $\gamma$  is the gyromagnetic ratio for the  $^1\text{H}$  nuclei,  $r$  is the proton-proton separation,  $\hbar = h/2\pi$  where  $h$  is Planck's constant,  $\tau_c$  is the correlation time of the

random reorientation, and  $\omega_0$  is the resonance frequency of the proton spins. Our analyses of the data were carried out by assuming a maxima in  $T_1^{-1}$  when  $\omega_0 \tau_c = 0.616$ , and that the BPP relation between  $T_1^{-1}$  and the characteristic frequency of motion  $\omega_0$  can be applied. Since the  $T_1^{-1}$  curves were found to exhibit a maximum, it was possible to determine the coefficient in the BPP formula. We were then able to calculate the parameter  $\tau_c$  as a function of the temperature.

The temperature dependence of  $\tau_c$  follows a simple Arrhenius expression

$$\tau_c = \tau_0 \exp(E_a/RT) \quad (3)$$

The slope of the straight-line portion of the semilog plot can be used to determine the activation energy,  $E_a$ . The activation energy for the molecular motion can be obtained from the  $\log \tau_c$  vs. the  $1000/T$  curve as shown in Fig. 3. The activation energy was found to be 3.76 kcal/mol.

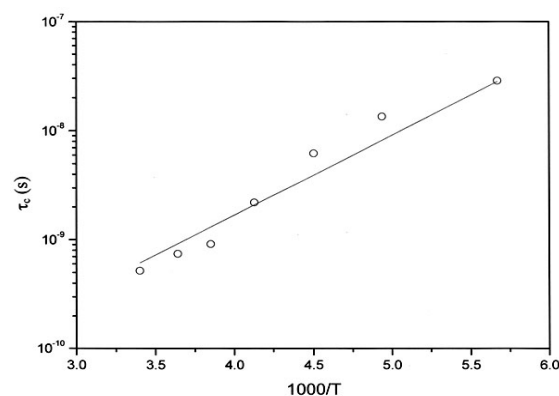


**Figure 3.** Arrhenius plot of the natural logarithm of the correlation time for proton as a function of the inverse temperature.

*Li<sub>2</sub>SO<sub>4</sub>·H<sub>2</sub>O single crystals*—The NMR line width for  $^1\text{H}$  is shown as a function of the temperature in Fig. 4. Temperature behaviors of the  $^1\text{H}$  line width for  $\text{Li}_2\text{SO}_4 \cdot \text{H}_2\text{O}$  single crystals show distinct trend associated with the molecular motion, compared to those for  $\text{LiH}_3(\text{SeO}_4)_2$  single crystals. As the temperature is increased, the line width decreases indicating increased molecular motion. The Gaussian line shape below 125 K changed into Lorentzian

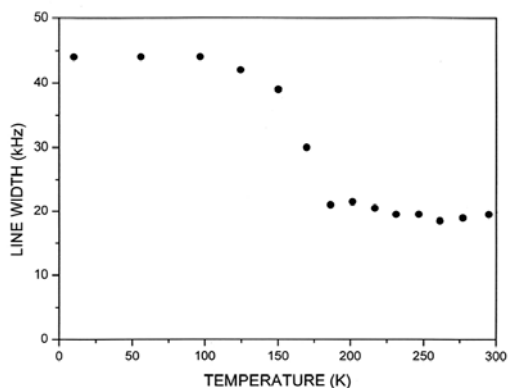


**Figure 4.**  $^1\text{H}$  NMR line-width as a function of temperature for a  $\text{Li}_2\text{SO}_4\cdot\text{H}_2\text{O}$  single crystal.

shape at temperature above 185 K.

The spin-lattice relaxation rate  $T_1^{-1}$  was determined in the temperature range of 170 to 300 K. A plot of  $\log T_1^{-1}$  vs. inverse temperature is shown in Fig. 5. The maximum observed at 253 K has a well-defined BPP shape and, in this temperature range, is characteristic of the effect of molecular motion. At 170 K,  $T_1^{-1}$  is  $6.90 \text{ ms}^{-1}$ , the lowest value obtained in this study. As the temperature increases,  $T_1^{-1}$  increases until it reaches a maximum of  $5.55 \text{ s}^{-1}$  at 253 K; at higher temperatures it decreases with increasing temperature. This result is consistent with the trends found for  $T_1^{-1}$  for  $^1\text{H}$  nuclei in  $\text{NH}_4\text{H}_2\text{PO}_4$  and  $\text{NH}_4\text{SCN}$  single crystals.<sup>14, 15</sup> The values of  $\tau_c$  were calculated from Eq. (2). The slope of the straight-line portion of the semilog plot was used to determine  $E_a$ , i.e. from a slope of the  $\log \tau_c$  vs. the  $1000/T$  curve, as shown insert Fig. 5. The activation energy for the molecular motion was 7.81 kcal/mol. This value is consistent with previously reported values.<sup>14</sup> The  $^1\text{H}$  nuclei in  $\text{Li}_2\text{SO}_4\cdot\text{H}_2\text{O}$  undergo molecular motion with an activation energy of 7.81 kcal/mol.

*LiN<sub>2</sub>H<sub>5</sub>SO<sub>4</sub> single crystals*– Fig 6. shows the FWHM of the NMR line width for  $^1\text{H}$  in  $\text{LiN}_2\text{H}_5\text{SO}_4$  as a function of the temperature.

As the temperature decreases, the line width increases in step-like fashion, reaching a rigid lattice value at lower temperatures. This stepwise narrowing is generally considered to be caused by internal motions that have a temperature dependence connected with that observed for the line width.<sup>8</sup>

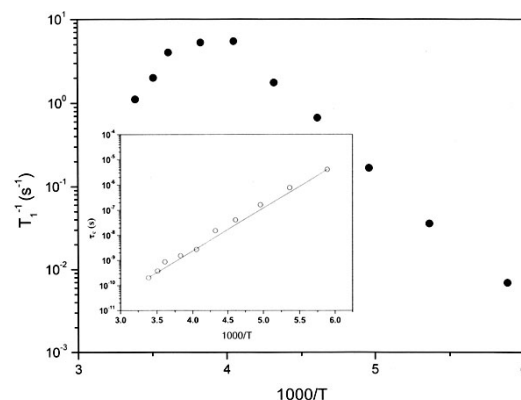


**Figure 5.** Temperature dependence of the spin-lattice relaxation rate,  $T_1^{-1}$ , for  $^1\text{H}$  in a  $\text{Li}_2\text{SO}_4\cdot\text{H}_2\text{O}$  single crystal. (inset: Arrhenius plot of the natural logarithm of the correlation time for proton as a function of the inverse temperature)

When the temperature increases, the shape of the line changes, progressing from the Gaussian-like shape produced by a rigid lattice to a Lorentzian shape. At low temperatures, the line width of  $^1\text{H}$  is less for  $\text{Li}_2\text{SO}_4\cdot\text{H}_2\text{O}$  crystals than for  $\text{LiN}_2\text{H}_5\text{SO}_4$  crystals.

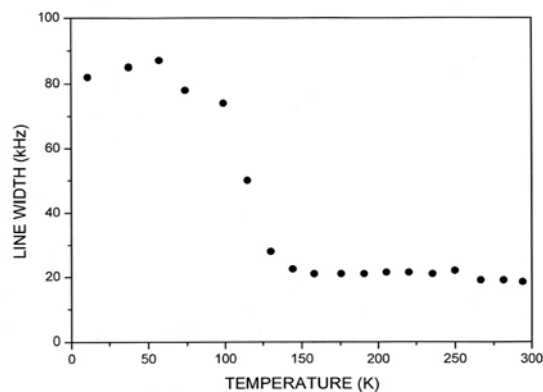


**Figure 6.**  $^1\text{H}$  NMR line-width as a function of temperature for a  $\text{LiN}_2\text{H}_5\text{SO}_4$  single crystal.

The proton spin-lattice relaxation rate was measured in the temperature range 100–300 K. These results similar to the trend of  $T_1$  for the  $^1\text{H}$  nucleus in  $\text{Li}_2\text{SO}_4\cdot\text{H}_2\text{O}$  single crystals. This feature of  $T_1$  indicates that distinct molecular motion is present. The form of the proton  $T_1$  vs. inverse temperature curve leads us to believe that the relaxation process is caused by the  $\text{N}_2\text{H}_5$  motion. The main feature of these results is the maximum in  $T_1^{-1}$  at 190 K. The

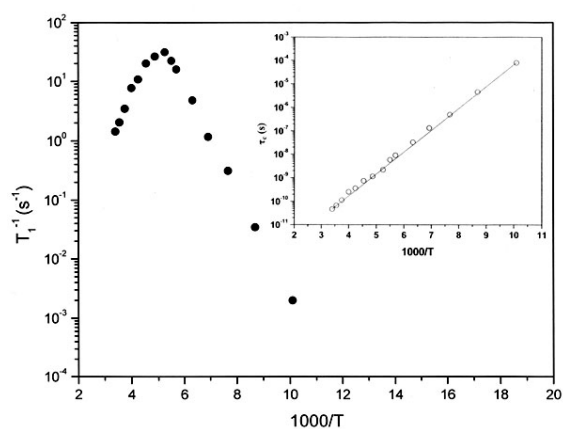


**Figure 7.** Temperature dependence of the spin-lattice relaxation rate,  $T_1^{-1}$ , for  $^1\text{H}$  in a  $\text{LiN}_2\text{H}_5\text{SO}_4$  single crystal. (inset: Arrhenius plot of the correlation time as a function of inverse temperature for protons)

activation energy for the molecular motion can be obtained from the  $\log \tau_c$  vs. the  $1000/T$  curve as shown insert of Fig. 7. The activation energy was found to be 4.23 kcal/mol. This value is consistent with previously reported values.<sup>17-19</sup>

## Discussion and Conclusions

The proton NMR line widths and spin-lattice relaxation rates of the  $\text{LiH}_3(\text{SeO}_3)_2$ ,  $\text{Li}_2\text{SO}_4 \cdot \text{H}_2\text{O}$ , and  $\text{LiN}_2\text{H}_5\text{SO}_4$  single crystals were measured. The line widths and spin-lattice relaxation rates were found to be greatly influenced by the environment of proton and by the mobility of the proton nuclei. The temperature dependences of the proton spin-lattice relaxation rates for these crystals have maximum

values, a fact which is attributable to the effects of molecular motion. Our results for  $\text{Li}_2\text{SO}_4 \cdot \text{H}_2\text{O}$  and  $\text{LiN}_2\text{H}_5\text{SO}_4$  crystals are consistent with those of previous reports,<sup>16-19</sup> whereas our results for  $\text{LiH}_3(\text{SeO}_3)_2$  crystals are not consistent with those of previous report.<sup>11</sup> The experimental results were analyzed using the BPP<sup>7</sup> relaxation theory. The activation energies for the molecular motions of  $^1\text{H}$  in  $\text{LiH}_3(\text{SeO}_3)_2$ ,  $\text{Li}_2\text{SO}_4 \cdot \text{H}_2\text{O}$ , and  $\text{LiN}_2\text{H}_5\text{SO}_4$  single crystals were found to be 3.76, 7.81, and 4.23 kcal/mol, respectively. The activation energy for  $^1\text{H}$  spin-lattice relaxation in  $\text{LiH}_3(\text{SeO}_3)_2$  crystals has a small value, whereas in  $\text{Li}_2\text{SO}_4 \cdot \text{H}_2\text{O}$  crystals it has a larger value. From these results, we conclude that the H-O hydrogen bond in  $\text{Li}_2\text{SO}_4 \cdot \text{H}_2\text{O}$  is stronger than the N-H hydrogen bond in  $\text{LiN}_2\text{H}_5\text{SO}_4$ , and that the H-O-Se hydrogen bond in  $\text{LiH}_3(\text{SeO}_3)_2$  is weaker than the H-O hydrogen bond in  $\text{Li}_2\text{SO}_4 \cdot \text{H}_2\text{O}$ . We deduce that the  $^1\text{H}$  nuclei in  $\text{LiH}_3(\text{SeO}_3)_2$  crystals undergo molecular motion more easily than  $^1\text{H}$  nuclei in  $\text{Li}_2\text{SO}_4 \cdot \text{H}_2\text{O}$  and  $\text{LiN}_2\text{H}_5\text{SO}_4$  crystals.

The characteristic of the protonic conductor may be due to the transfer of the proton within the hydrogen bond and breaking of the hydrogen bond together with the reorientation of the ionic group involved in the hydrogen-bond formation. The activation energy for H-O-Se hydrogen bond in  $\text{LiH}_3(\text{SeO}_3)_2$  crystals obtained here is very small, therefore, the transfer of the proton within the hydrogen bond and breaking of the hydrogen bond in high temperature is expected. From these result, the  $\text{LiH}_3(\text{SeO}_3)_2$  crystal in three crystals may be have high possibility as the protonic conductor material.

## References

1. P. Colomban and A. Novak, *Anhydrous Materials, Oxonium Perchlorate, Acid Phosphates, Arsenates, Sulphates and Selenates in Proton Conductors*, Cambridge University Press, Great Britain, 1992.
2. R. Kubo and K. Tomita, *J. Phys. Soc. Japan.* **9**, 888 (1954)
3. G. Burns, *Phys. Rev.* **123**, 64 (1961)
4. S. R. Miller, R. Blinic, M. Brenman, and J. S. Waugh, *Phys. Rev.* **126**, 528 (1962)
5. A. R. Lim, J. K. Jung, and S.Y. Jeong, *Solid State Commun.* **118**, 453 (2001)
6. J. L. Koenig, *In Spectroscopy of Polymers*, Elsevier Science Inc., New York, (1999)
7. N. Bloembergen, E. M. Purcell and R. V. Pound, *Phys. Rev.* **73**, 679 (1948)
8. A. Abragam, *The Principles of Nuclear Magnetism*, Oxford University Press, Oxford, (1989)

9. A. R. Lim and K.-S. Lee, *J. Kor. Mag. Reson. Soc.* 19, **29** (2015)
10. S. J. Lee and A.R. Lim, *J. Kor. Mag. Reson. Soc.* 19, **18** (2015)
11. A. A. Silvidi, *J. Chem. Phys.* **48**, 1402 (1968)
12. C. P. Slichter, *Principles of Magnetic Resonance*, Springer-Verlag, New York (1989)
13. B. Cowan, *Nuclear Magnetic Resonance and Relaxation*, Cambridge University Press, Cambridge, (1997)
14. R. Ikeda and C. A. McDowell, *Molecular Physics* **25**, 1217 (1973)
15. J. A. Ripmeester and N. S. Dalal, *Phys. Rev. B.* **18**, 3739 (1978)
16. D. F. Holcomb and B. Pedersen, *J. Chem. Phys.* **36**, 3270 (1962)
17. J. D. Cuthbert and H. E. Petch, *Can. J. Phys.* **41**, 1629 (1963)
18. W. D. MacClement, M. Pintar, and H. E. Petch, *Can. J. Phys.* **45**, 3257 (1967)
19. R. R. Knispel and H. E. Petch, *Can. J. Phys.* **49**, 870 (1971)